A Letters Journal Exploring the Frontiers of Physics

November 2013

EPL, **104** (2013) 48002
doi: 10.1209/0295-5075/104/48002

www.epljournal.org

Predicting self-terminating ventricular fibrillations in an isolated heart

Duy-Manh Le[1,3], Alexey V. Dvornikov[2,4], Pik-Yin Lai[1,2] and C. K. Chan[1,2]

[1] *Department of Physics and Center for Complex Systems, National Central University Chungli, Taiwan 320, R.O.C.*
[2] *Institute of Physics, Academia Sinica - Nankang, Taipei, Taiwan 115, R.O.C.*
[3] *Institute of Physics, VAST - 10 Dao Tan, Ba Dinh, Hanoi, Vietnam*
[4] *Department of Cell and Molecular Physiology, Loyola University School of Medicine 2160 South First Ave., Maywood, IL 60153, USA*

received 30 April 2013; accepted in final form 15 November 2013
published online 9 December 2013

PACS 87.19.Hh – Cardiac dynamics
PACS 82.39.Rt – Reactions in complex biological systems
PACS 05.10.-a – Computational methods in statistical physics and nonlinear dynamics

Abstract – Ventricular fibrillations (VFs) in isolated hearts induced by fast pacing are studied in a Langendorff preparation by measuring the electrical signals from the right atrium (V_a) and the ventricle (V_v). We find that when there is a strong component of V_v detected in V_a during VF, the induced VFs are usually not self-terminating. Criteria for the prediction of self-terminating VFs are developed based on the analysis of V_v and V_a by the cross-wavelet power spectrum and cross-Fourier power spectrum methods. The success rate of our prediction criteria is about 80–90%. Our findings suggest that a heart under VF can recover its sinus rhythm only when the sino-atrial node of the heart is not under strong influence of the VF from its ventricle.

Introduction. – Ventricle fibrillation (VF) refers to the situation of uncoordinated contraction of the cardiac muscle of the ventricles in the heart, resulting in no or very small contraction pressure of the ventricular chambers [1]. VF is known as the major cause of the cardiac sudden death [2]. In vertebrate hearts, the contraction signals are sent from the pacemaker, sino-atrial (SA) node in normal conditions, to different parts of the heart in the form of excitation waves via the conduction system. For blood to be pumped properly, different parts of the heart perform orchestrated contraction under the control of the SA node. However, during VF, the contraction of the heart is no longer controlled by the SA node but instead undergoes randomly localized re-excitations (such as spirals or broken spirals) [3]. Since these re-entrant excitations have much higher frequencies than that of the SA node, the signal from the SA node cannot propagate to different parts of the heart and the blood flow will stagnate.

In most models of excitable media, it is impossible for a heart under VF to return to its sinus rhythm without external interventions. Many simulation studies have been devoted to develop pacing or control schemes [4,5] to return the heart to its sinus rhythm. Up till now, the most practical solution of external interventions is to use an electrical defibrillator to reset all the local re-entrant excitations in the heart and then wait for the SA node to take over the control again and restore the heart to its sinus rhythm. However, in some rare documented cases, patients with VF are able to recover without any external interventions [1]. This phenomenon is know as self-terminating VF (STVF) [6,7] or transient VF [8]. A thorough understanding of the mechanism of STVF is of vital importance for both clinical applications and understanding of dynamics of excitable systems, in particular the attenuation of spiral waves [9]. The ability to control VF by turning the sustained VF into self-terminating VF by means of drugs or implants is a big challenge for clinicians. However, the basic mechanism of STVF is still far from clear.

As a first step to understand the mechanism of STVF, one essential question would be: is there any sign from the measured ECG which can be used to distinguish between cases of STVF and non-STVF? For this issue, Clayton *et al.* [6] used the Fourier transform to study the dominant frequency and peak size of the power spectrum of ventricle ECG of the VFs that were measured from

patients. However, because of the limitation of available data, the findings in ref. [6] remained to be verified. In this paper, we report results from isolated heart experiments which are carried out to answer this question. In our experiments, electrical signals measured at two locations, one very close to the SA node (V_a) on the right atrium (RA) and the other one (V_v) from the ventricle of a heart under VF, are analyzed to search for the sign to distinguish between STVF and non-STVF. Our results lead to the hypothesis that STVF is possible only when the signals from the SA node (through the RA) are not strongly affected by the VF in the ventricle. The analysis is carried out by the cross-wavelet power spectrum [10] and cross-Fourier power spectrum. In most cases, STVF cannot occur when V_a contains a significant amount of harmonics from V_v. Intuitively, the amount of V_v in V_a can then be used as a criterion to distinguish between STVF and non-STVF. With this criterion, a success rate of more than 80% is observed in our experiments.

Experiments. – Our induced VF experiments are carried out in isolated rat hearts perfused in a Langendorff system with Krebs-Henseleit (KH) buffer. Briefly, the Langendorff system is used to maintain the physiological condition of an isolated heart and keeping it functional by providing perfusion with nutrient-rich and oxygenated solution at a constant temperature (37 °C). In our experiments the hearts are extracted from Wistar rats (weight between 250 g to 300 g and normal heart rate of 3–6 Hz, both males and females). Usually an experiment can last for three to four hours. Two bipolar pseudo-ECGs, one from the RA (very close to the SA node) and the other one from the apex, are monitored by inserting the electrodes in the heart tissues. The idea is to use these two signals to look for the difference in STVF and non-STVF. The signal from the RA (V_a) is used to represent the dynamics of the RA which should still be controlled by signals from the SA node if the VF is not dominating the whole heart while V_v is the signal from the ventricle. A pacing electrode placed on the septum between the two ventricles is used to provide controlled stimulation to the heart. The contraction pressure of the left ventricle (LVP) is monitored by a water-filled balloon inserted into the chamber via the left atrium and connected to a pressure transducer. VF in isolated hearts perfused with KH buffer can be induced by fast pacing (20 to 62.5 Hz). Detailed descriptions of our setup and experimental conditions can be found in ref. [11,12]. The protocols of the present study were approved by the Board of Ethics of Academia Sinica and conducted according to the National Institute of Health Guidelines for the Use and Care of Laboratory Animals [13].

Figure 1(a) shows a typical scenario of induced VF by fast pacing in hearts perfused with regular KH buffer, the VF lasted for a long time and was regarded as non-STVF. Figure 1(b) shows another scenario of the spontaneous termination of VF (STVF). In these figures, three signals

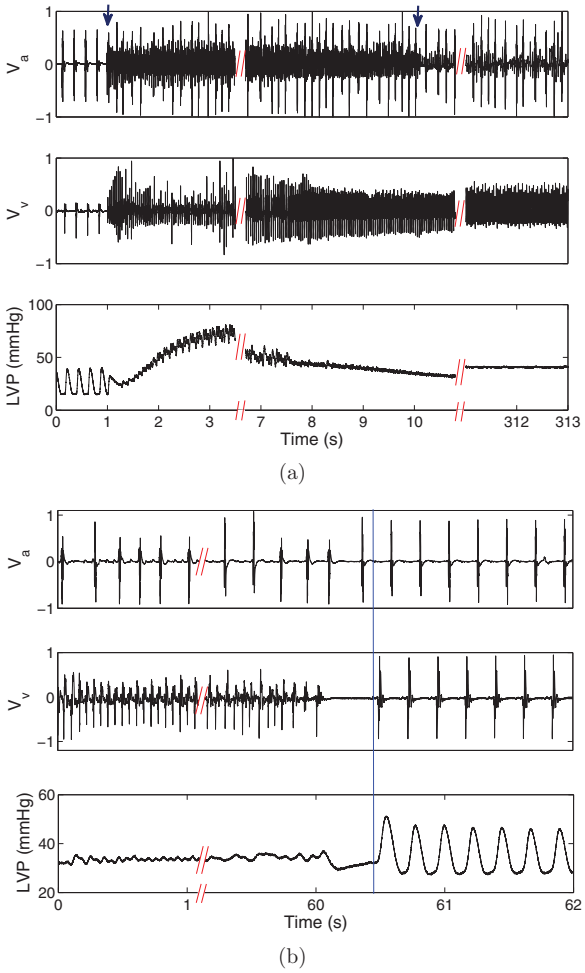

Fig. 1: (Color online) Time courses of V_a, V_v and LVP of typical non-STVF and STVF under normal KH buffer. Notice the low activity of LVP during VF. (a) Non-STVF. Normal rhythm is shown from 0 to 1 s. VF is induced by fast pacing (at 62.5 Hz from $t = 1$ to 10 s indicated by two blue arrows on the top panel), VF occurs at $t \sim 7.8$ s which can be visualized by the qualitative change in LVP. VF lasted for more than 5 minutes. (b) A STVF episode. Note that STVF occurs (indicated by the vertical blue line) after VF for more than a minute.

are shown; namely V_a, V_v and LVP. In our experiments, episodes of VF are identified with the following criteria: (a) fast (4 to 10 times faster than normal beating rate) turbulent oscillations in V_v (the frequencies of these turbulent oscillations range from 12 to 50 Hz in all our observed VF episodes) and (b) very small variations of LVP (about 20 or more times smaller than normal) as shown in the figures. In our experiments, if the VF disappears within 5 minutes by itself, the VF is considered as STVF (fig. 1(b)); otherwise it is identified as non-STVF. In the cases of non-STVFs, VFs are terminated by intra-coronary injection of lidocain (0.2 ml, 10 mM) to save the heart for the next experiment. In our experiments, a total of 29 VF episodes under normal KH buffer are collected from 11 isolated rat hearts in which 17 episodes are STVFs

and the other 12 episodes are non-STVFs. In order to test the validity of our analysis of the dynamical signatures for STVF and non-STVF presented below, we have also performed experiments with KH buffer with high calcium concentration (HCB)[1]. There are 9 VF episodes from these HCB experiments. These HCB data are presented below to demonstrate that the validity of our analysis is independent of how the STVFs are induced.

Data analysis. – Our goal is to use data from the VF episodes to detect the characteristics of STVF. Presumably there are hidden relations between V_v and V_a which will enable the occurrence of STVF. Two data analysis methods, namely cross-wavelet spectrum (XWS) and cross-Fourier spectrum (XFS), are employed.

Wavelet power spectrum (WPS) and cross-wavelet spectrum (XWS). The wavelet transform is localized in both time and frequency, making it especially suitable for non-stationary time series. Consider an equal time spacing (δt) time series of N time points $X = \{x_n, n = 0, \ldots, N-1\}$, then the continuous wavelet transform (CWT) of X is defined as [14]

$$W_n^X(s) = \sqrt{\frac{\delta t}{s}} \sum_{n'=0}^{N-1} x_{n'} \Psi_0 \left[(n - n') \frac{\delta t}{s} \right], \qquad (1)$$

where $\Psi_0(\eta) = \pi^{-\frac{1}{4}} e^{i\omega_0 \eta} e^{-\frac{1}{2}\eta^2}$ is the mother wavelet function defined by the dimensionless frequency ω_0. η is the dimensionless time variable and $\omega_0 = 6$ for Morlet wavelet. s is the wavelet scale related to the Fourier frequency by $1/f = 1.03s$ for the Morlet wavelet. If we denote the CWT of X and Y time series by W^X and W^Y, respectively, then the cross-wavelet spectrum (XWS) of X and Y is given by $XWS_{XY} = |W^X W^{Y*}|$ where the $*$ denotes the complex conjugate. The XWS provides the time-frequency visualization for the common power of the X and Y signals revealing their inter-relation. The wavelet power spectrum (WPS) of one time series, say X, is also similarly defined: $WPS_X = |W_X|^2$. By using the XWS of bivariate signals, one can detect the co-existence modes of two time series that are believed to have interrelation and their corresponding strengths. A Matlab package [14] is adapted for the computation of WPS and XWS.

Fourier power spectrum (FPS) and cross-Fourier spectrum (XFS). The discrete Fourier transform of the time series X is given by $F_X = \sum_{n=0}^{N-1} x_n \exp(-2\pi i f n \delta t)$, then the FPS of X is given by $FPS_X \equiv \frac{4}{N^2}|F_X|^2$. Let F_Y denote the discrete Fourier transform of the time series Y of the same length (N time points), then the XFS of the time series X and Y is given by $XFS_{XY} = \frac{4}{N^2}|F_X F_Y^*|$. In fact, the XFS of X and Y is simply the forward Fourier transform of the cross-correlation function of X and Y [15]. That is why XFS can be used to detect the correlation between two time series. The highest power of the spectrum (FPS or XFS), referred to as the dominant power, occurs at the corresponding dominant frequency. The dominant power of the XFS is used to quantify the relation between the RA and ventricle signals in our analysis, and indicates the mode at which these two signals are most related at the corresponding dominant frequency. In our results, usually the dominant frequency of the XFS between RA and ventricle is close to that of the ventricle signal. Notice that signals V_a and V_v are all normalized to have unit standard deviation and amplitude in XWS and XFS methods, respectively, in order to facilitate comparisons between different episodes. Typical results for XWS and XFS are, respectively, shown in figs. 2, 3 and 4, and fig. 5 summarizes the dynamical signatures for STVF and non-STVF.

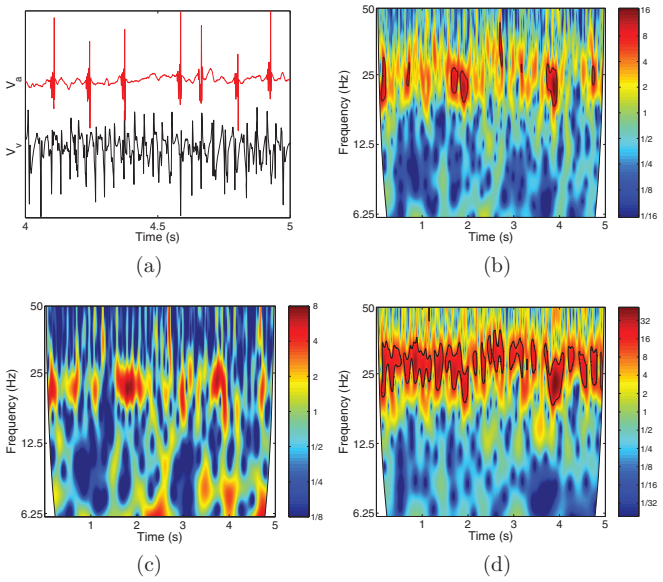

Fig. 2: (Color online) Wavelet spectrum analysis of a typical STVF episode under normal KH buffer. (a) Time series of RA (V_a, top red line) and ventricle (V_v, bottom black line) with the duration of the last second before VF is self-terminated. (b) Time-frequency plot showing the color-coded power of the XWS of the RA and ventricle signals. Results are shown for the last 5 second before recovery points. (c) WPS of the RA signal, and (d) WPS of the ventricle signal. In each time-frequency plot, significance tests are carried out on the wavelet spectra to remove spurious power [14,16]. The black contour shows the 5% significant level against noise, and the white areas are affected by the edge effect in the wavelet transform and they are excluded.

Results. – In the STVF episodes we observed, the duration of an episode lasts from 10 s to 275 s, but most of them occur in less than two minutes. Since the XFS method is not suitable for analyzing non-stationary data, only the last 5 seconds of data before the recovery of the

[1]The normal Krebs-Henseleit buffer contains 2.0 mM of calcium. Experimentally, we find that the HCB can induce VFs spontaneously and these induced VFs are usually short STVFs. The calcium concentration is 4 or 5 mM in HCB experiments. Higher concentration (5 mM) of calcium would be used when no STVF can be observed when the 4 mM buffer is used.

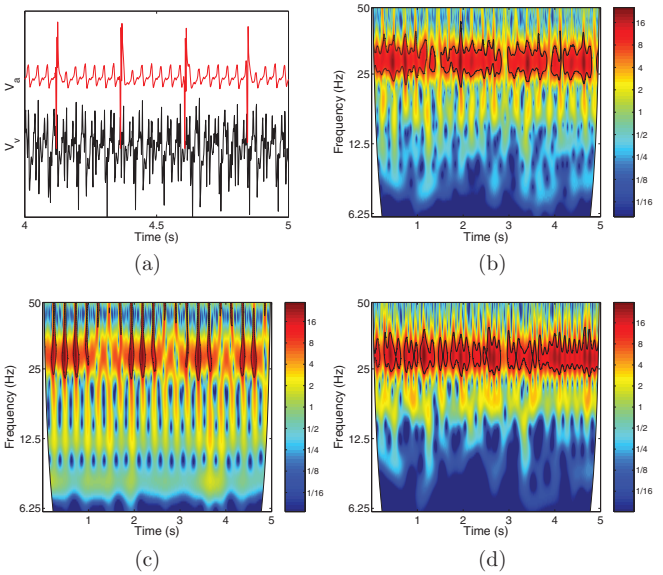

Fig. 3: (Color online) Wavelet spectrum analysis of a typical non-STVF episode under normal KH buffer. (a) Time series (1 second duration) of RA and ventricle signals after 5 minutes under VF. (b) XWS of the RA and ventricle signals. (c) WPS of the RA signal, and (d) WPS of the ventricle signal.

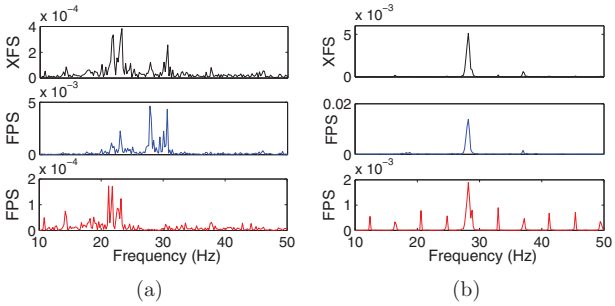

Fig. 4: (Color online) Fourier spectrum analysis of STVF and non-STVF episodes under normal KH buffer. (a) A typical STVF episode. The top, middle, and bottom panels correspond to the XFS of V_a and V_v, the FPS of V_v, and FPS of V_a, respectively. In this episode, the dominant frequency of the XFS is about 23 Hz corresponding to the third strongest components of both FPSs of V_v and V_a. (b) A typical non-STVF. The arrangement of each panel is similar to that of (a). The dominant frequencies of both V_v and V_a are about 28 Hz, resulting in the same dominant frequency of the XFS with a high dominant power.

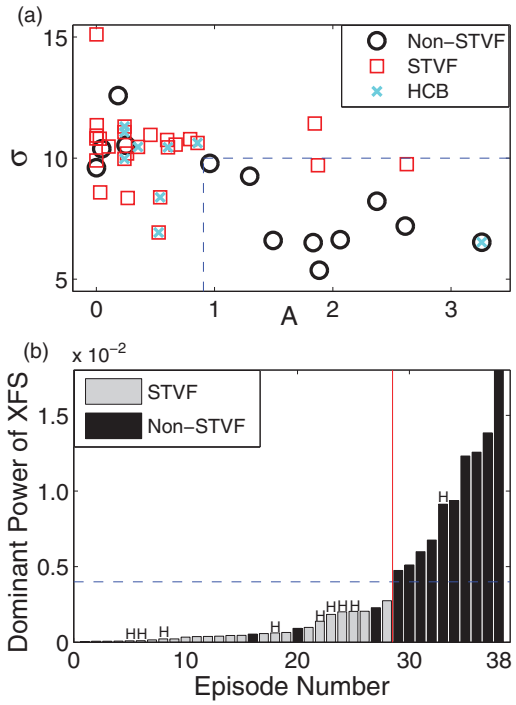

Fig. 5: (Color online) Summary of the dynamical signatures of STVFs and non-STVFs using XWS and XFS analyses. Twenty-nine episodes of VFs under normal KH buffer, and 9 episodes of VFs under HCB conditions (marked with × in (a) and labeled by "H" in (b)). A total of 38 VF episodes from 11 hearts, comprising 25 STVF and 13 non-STVF scenarios. (a) Standard deviation, σ, of $P(f)$ *vs.* the total area A enclosed by the black contours (5% significance level). See text for the explanation of the dashed lines. (b) The dominant power of XFS of the RA and ventricle signals. The blue dashed horizontal line denotes the XFS value of 0.004, which can serve as a guide to distinguish STVFs and non-STVFs into two groups separated by the vertical red line.

sinus rhythm are used for the analysis of STVF and the last 5 seconds of the first 5 minutes of VF are used in the case of non-STVF. From our observations, we believe that signals are quasi-stationary in this short time window. On the other hand, the wavelet method can handle these non-stationary data well and there is no restriction to short time windows. However, in order to have a consistent comparison with the XFS method, we also used the last 5 seconds window. The original data are recorded at a sampling rate of 4 kHz. We have tested that results reported below will not be substantially changed even when the data are down-sampled from 4 kHz to 400 Hz by data point skipping. For the wavelet method, different sampling rates only slightly change the time-frequency wavelet spectrum plots. The general features are the same.

Wavelet power spectrum. To demonstrate the differences in the signals of V_v and V_a from STVF and non-STVF episodes, the time course of these signals from typical episodes are shown in fig. 2(a) and fig. 3(a), respectively. A remarkable feature of these time traces is that one can clearly see the signal of V_v in V_a in the case of non-STVF. Special cares have been exercised to ensure that there is no electrical cross-talk between these two signals due to electrical couplings of cables or amplifiers. This feature suggests that the dynamics of the RA is under the strong influence of the VF in the ventricle for non-STVF; but it is not so in STVF. Since V_a is taken very close to the SA node, presumably a similar effect might also be taking place in the SA node. This leads us to hypothesize that

self-termination of VF fails because of the strong effect of the ventricle signal on the SA node.

To quantify the effects of the influence of the fibrillations in the ventricle on the RA, the corresponding XWS (between V_v and V_a) and WPS are also shown in fig. 2 (SVTF) and fig. 3 (non-STVF). The influence can be characterized by the XWS and the distribution of these powers over different frequencies. The area of 5% significant power [16] in the spectrum is enclosed by black contours to indicate regions of strong power. The total area (A) enclosed by these black contours in the frequency range of 12–50 Hz provides a measure of the strength or significance of the wavelet spectrum. Notice that we choose this range of frequency to quantify the relation between V_v and V_a because it is the frequency range of fibrillation captured in our data for all samples. The distribution of this strength in frequency can be measured by the standard deviation, σ, of the frequency distribution $P(f)$ which is the time average of the XWS. A small σ indicates that these powers are concentrated in a small frequency range and vice versa.

Figure 5(a) shows the results of using A and σ to characterize the influence of V_v on V_a for all the VF episodes in our experiments. It can be seen from fig. 5(a) that for the 29 VFs under normal KH buffer, most of non-STVFs fall into a region with $A > 0.9$ and $\sigma < 10$ and most of STVFs are outside this region. It should be noted that earlier applications of wavelet approaches to ECG data have also associated high spectral power concentrated in a narrow frequency range with cardiac pathologies [17,18], instead of fractal-like cascades for typical healthy conditions. We find that 15 out of the 17 STVF episodes have either small A or large A together with a large σ as depicted in fig. 5(a). Also, 9 out of the 12 non-STVF episodes are characterized by large A and small σ. If we use the criteria of large A and small σ, the region bounded by the dashed lines in fig. 5(a), for predicting non-STVF, the success rate is $8/10 = 80\%$. And using the criteria of small or A is large but with large σ (outside the dashed rectangle) to predict the occurrence of STVF, the success rate is $15/19 = 79\%$. The above observation remains valid for the VFs under HCB conditions (9 episodes marked by blue $\times$): all 8 STVFs lie outside the dashed box in fig. 5(a) while the non-STVF lies inside, *i.e.* 100% success rates for both STVF and non-STVF prediction. Therefore, regardless of the buffer conditions or the cause of VF, the criteria of large A and small σ appears to be an accurate indicator for non-STVF, and STVF is associated with small A or large A but with large σ (outside the dashed box). If we take all 38 VF episodes into account, the success rate is about 82% for predicting non-STVF (region bounded by the dashed box in fig. 5(a)), and the successful rate for STVF prediction is about 85%.

Fourier power spectrum. The FPS and XFS of V_a and V_v of fig. 2 and fig. 3 are shown in fig. 4(a) and (b), respectively for the case of STVF and non-STVF. Typically, the non-STVF spectra show localized frequency bands while the STVF spectra are more continuous, and the magnitudes of the STVF spectra are about an order magnitude smaller. Furthermore, the V_a of STVFs have a widely distributed FPS as shown in the bottom panel of fig. 4(a). Since the power is distributed over a broad frequency range, its amplitude is small. Notice that the FPS of V_v is usually localized at some frequency (middle panel of fig. 4(a)) close to the frequency of fibrillation. This leads to the small dominant power in the XFS (top panel of fig. 4(a)). Contrary to the STVFs, FPS of V_a from the non-STVF episodes are characterized by higher powers at some harmonics of the RA rhythm for the case that its own beating is quite regular and highly nonlinear (bottom panel of fig. 4(b)), and the power of the FPS of V_v is highly localized around the frequency of fibrillation (middle panel of fig. 4(b)). As a result, the dominant power in the XFS of non-STVF episodes becomes very high in comparison to that of STVF.

Figure 5(b) is a summary of the values of the dominant power of the XFS for all the VF episodes. The group of STVFs is shown in gray and the non-STVF group is shown in black. For the 29 VFs under normal KH buffer, all of the 17 STVFs possess small dominant XFS values (say lower than 0.004). And 9 out of the 12 non-STVFs possess large dominant XFS values (> 0.004). This chart suggests that VF with a high dominant XFS power has little chance for self-terminating, whereas the VF with a low dominant power has a very good chance to recover to its normal rhythm. It can be seen easily from fig. 5(b) that there are two well-separated groups as marked by the vertical line. The first group is characterized by low dominant power (< 0.004). For VF episodes under normal KH buffer, the group on the left in fig. 5(b) (having XFS values < 0.004) contains a total of 20 episodes out of which 17 are STVF. Thus, it is clear that the VF episodes with a low dominant XFS power have higher chances ($\sim 85\%$) to survive. The second group is characterized by high dominant power (> 0.004). It contains 9 episodes and all of them are non-STVF (100%). Such a dynamical signature is also confirmed by the 9 VF episodes under HCB conditions: all of the 8 STVFs have small dominant XFS power and that of the non-STVF is large. Hence, the XFS analysis also indicated that regardless of the cause of VF, VF has little or no chance to self-terminate when the dominant power of XFS is high. Using all 38 VF episodes and the dividing line of high and low dominant power of XFS in fig. 5(b), the success rates for predicting STVF and non-STVF are 89% and 100%, respectively.

Discussions. – From the statistical results discussed above, it is clear that both the XWS and XFS methods are valid indicators for STVF or non-STVF. Both of these results support our hypothesis that there are correlations between V_a and V_v around the frequencies of fibrillation, as manifested in the case of non-STVF displaying significantly strong XWS or high XFS dominant power. The above observations remain valid regardless of

the conditions of VF, for hearts under normal KH buffer as well as under HCB conditions. Actually, one can see that the ventricle mode appeared rather prominently in the RA signal, as shown in fig. 3(a). During VF episodes, since the RA is still beating more or less with the sinus rhythm while the ventricle is beating much faster, one can safely assume that the dynamics of the RA is still controlled by the SA node. That is: the fast electric excitations from the ventricle cannot reach the RA. However, there must be some additional form of coupling to induce a V_v component in V_a.

One possible origin of this coupling is the mechanical coupling via fibroblasts in the heart which are mechanical sensitive [19]. If this is the case, the existence of the component of V_v in V_a for non-STVF suggests that the mechanical stresses generated by VF in the ventricle can be felt by the fibroblasts in the RA. As the measuring point of the V_a is very close to the SA node, these mechanical stresses should also be felt by the SA node. If the coupling is mechanical in nature, there is a good possibility that the dynamics of the SA node will be affected because it is known that mechanical stresses can alter the dynamics of the SA node [20]. In this scenario, the VF in the ventricle can alter the dynamics of the SA node; in contrast to the usual condition under which the SA node is sending signals to control ventricular contraction. Thus, the SA node can sustain its own activity only when there is no significant amount of V_v in the measured V_a; our criterion for STVF. With this picture, a non-STVF episode cannot recover because the SA node is then under the strong influence of the VF in the ventricle. Presumably, one needs a normally functioning SA node to provide the sinus rhythm for recovery.

Recently Biktashev *et al.* [21,22] has proposed that the dissipation of excitation wave fronts in cardiac tissues can be the origin of self-terminating fibrillation. In this model, the wave front of excitations can no longer propagate because the wave fronts are broken by an instability due to dissipations. In such a situation, the fibrillation is terminated by dynamics of these nonpropagating wave fronts. Since there is no SA node and the atrial tissue is considered in these studies, it would be very interesting to see if our results presented here can be reproduced in their model when the dynamics of the SA node is incorporated. An alternative mechanism for STVF may be related to the attenuation of spiral waves by low-frequency planar fronts [9], in which the planar fronts from the SA node can sustain its rhythm and eventually can terminate VF.

Finally, a peculiar feature of their model is that not only fibrillations can be self-terminating but they can also be spontaneously generated. This phenomenon is very similar to what we observed in some VF episodes under HCB. In ref. [22], the local dissipation of the wave front is associated with the inactivation of the sodium current. Since calcium can block and affect the closing rate of the sodium channel [23], the ability of HCB to generate spontaneous transient VFs might probably be related to this effect. It should be noted that despite the low sample statistics of 9 VF episodes under HCB, 8 of them showed STVF confirming that the Ca channel is important in STVF.

* * *

The authors would like to thank Prof. Zbigniew Struzik and Prof. Ming-Chya Wu for useful discussions. This work has been supported by the NSC of ROC under the grant Nos. NSC 100-2923-M-001-008-MY3, 101-2112-M-008-004-MY3, and NCTS of Taiwan.

REFERENCES

[1] Wigger C. J., *Am. Heart J.*, **20** (1940) 399.
[2] Karma A. and Gilmore R. F., *Phys. Today*, **60**, issue No. 3 (2007) 51.
[3] Qu Z. and Weiss J. N., *J. Cardiovasc. Electrophysiol.*, **17** (2006) 1042.
[4] Yuan G., Wang G. and Chen S., *Europhys. Lett.*, **72** (2005) 908.
[5] Osipov G. V., Shulgin B. V. and Collins J. J., *Phys. Rev. E*, **58** (1998) 6955.
[6] Clayton R. H., Murray A. and Campbell R. W. F., *Comput. Cardiol.* (1994) 705.
[7] van Hemel N. M. and Herre K. J., *Br. Heart J.*, **69** (1993) 568.
[8] Blaer Y. *et al.*, *Eur. J. Cardiovasc. Nurs.*, **6** (2007) 337.
[9] de la Casa Miguel A. *et al.*, *EPL*, **86** (2009) 18005; *Chaos*, **17** (2007) 015109.
[10] Hudgins L., Friehe C. A. and Mayer M. E., *Phys. Rev. Lett.*, **71** (1993) 3279.
[11] Dvornikov A. V., Mi Y. C. and Chan C. K., *Cardiovasc. Eng. Technol.*, **3** (2012) 203.
[12] Sridhar S., Le D. M., Mi Y. C., Sinha S., Lai P. Y. and Chan C. K., *Phys. Rev. E*, **87** (2013) 042712.
[13] National Research Council, *Guide for the Care and Use of Laboratory Animals* (National Academy Press, Washington, DC) 2011.
[14] Grinsted A., Moore J. C. and Jevrejeva S., *Nonlinear Processes Geophys.*, **11** (2004) 561; Matlab software package for performing wavelet and cross-wavelet transform, `http://noc.ac.uk/using-science/crosswavelet-wavelet-coherence`.
[15] Bracewell R. N., *The Fourier Transform and its Applications*, 3rd edition (McGraw Hill, Boston) 2000.
[16] Maraun D. and Kurths J., *Phys. Rev. E*, **75** (2007) 016707.
[17] Ivanov P. C. *et al.*, *Nature*, **383** (1996) 323; *Physica A*, **249** (1998) 587.
[18] Ivanov P. C. *et al.*, *Chaos*, **11** (2001) 641.
[19] Kamkin A. *et al.*, *Prog. Biophys. Mol. Biol.*, **82** (2003) 111.
[20] Horner S. M. *et al.*, *Circulation*, **94** (1996) 1762.
[21] Biktashev V. N., *Phys. Rev. Lett.*, **89** (2002) 168102; Aslanidi O. V. *et al.*, *Chaos*, **12** (2002) 843.
[22] Biktasheva I. V. *et al.*, *Int. J. Bifurcat. Chaos*, **13** (2003) 3645.
[23] Armstrong C. M. and Cota G., *Proc. Natl. Acad. Sci. U.S.A.*, **96** (1999) 4154.